Josephson junctions with ferromagnetic materials

M. Yu. Kupriyanov[1]*[a] , A.A. Golubov[b] , M.Siegel[c]
[a]Institute of Nuclear Physics, Moscow State University, Moscow, Russia;
[b]Faculty of Science and Technology, University of Twente, Enschede, The Netherlands
[c]Karlsruhe University, Institute of Micro- and Nanoelectonics Systems, Karlsruhe Germany

ABSTRACT

The current status of the material and interfaces aspects of the problem of SFS Josephson junction fabrication is reviewed and recommendations for selection of ferromagnetic materials are formulated. It is shown that additional pair braking mechanisms at SF interfaces, as well as spin flip and spin orbit scattering in the F films should be taking into account for the data interpretation. The results of theoretical studies of the influence of spin-flip and spin-orbit scattering on the oscillations of critical current with the thickness of the ferromagnetic layers are summarized and discussed. The form of the relation between supercurrent J and order parameters phase difference φ across a junction is analyzed. It is shown that the Josephson current across the structure has the sum of $\sin\varphi$ and $\sin 2\varphi$ components and that two different physical mechanisms are responsible for the sign of $\sin 2\varphi$.

Keywords: Josephson effect, proximity effect, SFS Josephson junctions

1. INTRODUCTION

In the past few years there was a noticeable interest to the unconventional Josephson junctions[1-3], in particular to the so-called π-junctions having negative critical current. These junctions provide the π- shift in the ground state and were realized experimentally in SFS (superconductor-ferromagnet-superconductor) and some HTS structures. Despite of intensive study of the processes in these structures there are several problems remained to be solved. They are influence of spin-flip and spin-orbit scattering on the oscillations of critical current with the thickness of the ferromagnetic layers; the form of the relation between supercurrent J and order parameters phase difference φ across a junction; spatial distribution of the critical current density in arrays of "0 and "π"-junctions. In this article we will briefly review the current status of these problems. We will start our analysis with the discussion of the properties of ferromagnetic materials, which could be used in SFS junctions. After that we switch on the theoretical models relevant for description of the phenomenon experimentally observed in this structures with the focus on the form of current phase relation.

2. BULK FERROMAGNETIC MATERIALS.

From the developed theoretical models for the description of the processes in SF/FS Josephson junctions[1-3] it is clearly seen that for the quantitative analysis of the experimental situations it is necessary to have an experimental information about both the material parameters of the metals (exchange field, decay and coherence length) and suppression parameters at all interfaces. Contrary to that recent experiments was mainly oriented on demonstration of the existence of some nonmonotonic dependencies of the critical current or gap in the density of states upon temperature or thickness of the F-layer rather than on systematic quantitative study of the structures. Below we will formulate recommendations, which, from our point of view, may be helpful for systematic experimental study of the SF/FS Josephson junctions and FS proximity systems.

[1] *mkupr@pn.sinp.msu.ru; phone (095) 9392588; fax (095) 9390896

Micro- and Nano-electronics 2005, edited by Kamil A. Valiev, Alexander A. Orlikovsky,
Proc. of SPIE Vol. 6260, 62600S, (2006) · 0277-786X/06/$15 · doi: 10.1117/12.681774

2.1. Bulk ferromagnetic materials.

The right choice of the ferromagnetic material for the structures is the important point. Our analysis[1] shows that the peculiarities in the SF/FS structures are located at ferromagnetic exchange energy $H \approx \pi T_c/\gamma_B$, where γ_B is an interface suppression parameter[1]. Taking into account that, as a rule, at SF interfaces $\gamma_B \approx 1$ we immediately see that H should be of the order or less then 30 K or 3 meV for low-Tc superconductors. Exchange energy in classical ferromagnetic materials, which has been extensively used for study the critical temperature of SF bilayers is considerably large (1 eV for bcc αFe, 0,61 eV for Gd, 0.13 eV for Ni). With this large values of H we are not only far from interval for observation of the effects, but have also the technological problems associated with the small values of decay length in ferromagnet. The predictions of existing theoretical calculations[1-3] is also not valued for the structures with these materials since the $H\tau$ product (τ is an electron elastic scattering time) may be not small, as it is necessary for making use of Usadel equation.

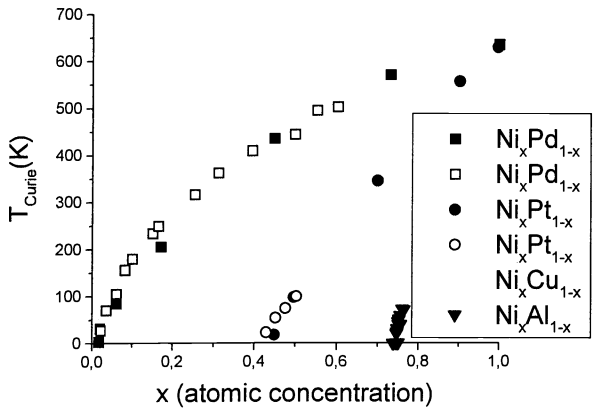

Figure 1: Dependence of the Curie temperature of ferromagnetic alloys on concentration of Ni. It is clearly seen that there are three classes of materials having small ($x \leq 0,1$), intermediate ($x \approx 0,5$) and large ($x \geq 0,7$) concentration respectively.

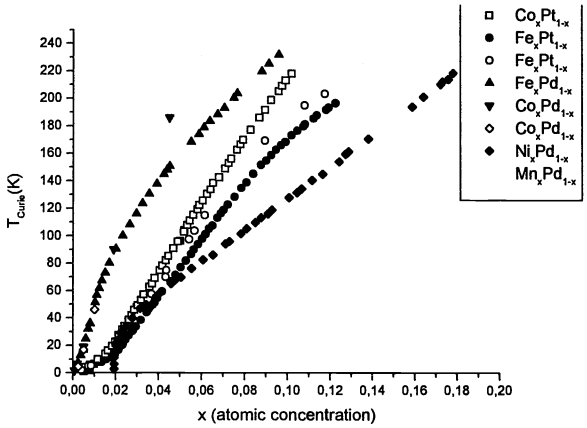

Figure 2: Dependence of the Curie temperature of ferromagnetic alloys on concentration of Co, Fe, Ni and Mn in Pt and Pd host materials.

Figure 1 gives the concentration dependence of the Curie temperature for a set of dilute ferromagnetic alloys and intermetallic compound. It is clearly seen that in the vicinity of critical concentration it is possible to reduce the Curie temperature to the values of the order of 30K. The second conclusion is that there are three classes of materials. They are the alloys with small critical concentration Ni_xPd_{1-x}, Fe_xPd_{1-x}, Co_xPd_{1-x}, Mn_xPd_{1-x}, Fe_xPt_{1-x}, Co_xPt_{1-x}, alloys with intermediate critical concentration Fe_xV_{1-x}, Ni_xPt_{1-x}, Ni_xCu_{1-x}, and intermetallic compound Ni_3Al with $T_{Curie} \approx 43$ K

2.1.1. Alloys with small critical concentration.

The evident advantage of using ferromagnetic alloys with small critical concentration of ferromagnet atoms in the weak link region is the possibility to perform the comparative study for the system with and without magnetic additions. At small level of x it seems that the transport properties of the host material will not change considerably with x increase in the range of few atomic percent. Therefore the difference between the properties of the structures with and without ferromagnetic atoms can be attributed to the influence of ferromagnet ordering or spin flip and spin orbit scattering rather than from changes of the host material transport properties.

The use Pd or Pt as the host provides the unique opportunity for realization of this approach. Platinum and palladium are typical exchange enhanced hosts that produce giant moment polarization in alloys in which the impurity is Fe, Co or Ni. Pt host has smaller exchange enhancement compare to Pd and Pt alloys have tended to be more complex, showing typical spin glass behavior at low impurity concentrations.

2.1.1.1. PdNi alloys

In the bulk, the NiPd alloys assumes as fcc structure and is known to exhibit ferromagnetic ordering down to a Ni concentration as low as 3 at%. Figures 1 and 2 demonstrate the summary of experimental $T_{Curie}(x)$ dependencies from[4-14] Ferromagnetic order in PdNi alloys results from an indirect exchange between the Ni magnetic moments provided by the large spin susceptibility of Pd. At low Ni concentrations, the total magnetic moment is mainly due to the spin polarized electrons of the host at the Fermi level. In the vicinity of critical concentration[9] $x_C \approx 0.026 \pm 0.002$, at which the ferromagnetic order is suppressed, $T_{Curie}(x) \approx (x - x_C)^{3/4}$, while at $x \geq 0.1$ at%, $T_{Curie}(x) \approx (x - x_C)^{1/2}$. The exchange energy $H \approx 15$meV and decay length $\xi_F \approx 45$ Å in $Pd_{0.9}Ni_{0.1}$ has been estimated in[15] from the experimental study of magnetization of $Pd_{0.9}Ni_{0.1}$/Nb multilayers and from the form of the density of states at free F surface in $Pd_{0.9}Ni_{0.1}$ /Nb sandwiches. From Josephson coupling in SIFS junctions[16] H was found to be equal to ≈35 meV resulting in nearly the same $\xi_F \approx 45$Å, under the value of suppression parameter $\gamma_B \approx 5.3$ at the $Pd_{0.9}Ni_{0.1}$/Nb boundary.

2.1.1.2. PdFe alloys

The ferromagnetic behavior of $Pd_{1-x}Fe_x$ alloys has been studied very intensively[17-30]. In $Pd_{1-x}Fe_x$, the Curie temperature T_{Curie} can be changed over a wide range of concentration x. In bulk alloys[22], ferromagnetism persists down to a concentration of about $x \approx 10^{-6}$ and T_{Curie} increases monotonically with increasing x up to $x \approx 10^{-4}$. In the interval $10^{-4} \leq x \leq 10^{-2}$ $T_{Curie} \sim x^{1,9}$, while at larger x there T_{Curie} again grows linearly with x. In thin films[26] with different thickness $d_F \approx 18$ A ($x \approx 0.05$); $d_F \approx 15$ A ($x \approx 0.13$); $d_F \approx 9$ A ($x \approx 0.2$) $d_F \approx 12$ A ($d_F \approx 0.2$) the T_{Curie} was equal to 60 K; 150 K; 70 K; 175 K respectively. These values are considerably smaller then them for the bulk alloys with the same concentration of Fe ($T_{Curie} \approx$ 162 K; 320 K; 440 K, respectively). Therefore there is the essential thickness dependence both of T_{Curie} and exchange energy. Note that for $x \approx 0.2$ the changes in thickness on 3 A only leads to the drastic changes in magnetic material constant of the ferromagnet. It was found, however, that at $x \geq 0.14$ effective decay length in $Pd_{1-x}Fe_x$, $\xi_F \approx 12$ A starts to be independent on Fe concentration with x increase. This can be the consequence of complex magnetic ordering in the alloy at $x \geq 0.14$ similar to that observed in $Pt_{1-x}Fe_x$ systems discussed below.

2.1.1.3. PdCo alloys

Like $Pd_{1-x}Fe_x$, $Pd_{1-x}Co_x$ is a giant moment ferromagnetic with a rather small critical concentration for ferromagnetism[31-33]. It was shown in[28] that homogeneous samples display a ferromagnetic transition typical of alloys, which develop hysteresis right at the Curie temperature. It was observed also that plastic deformation of Pd-Co samples increases their Curie temperature. This was thought to be due to changes in the degree of chemical clustering of Co atoms. Small gradients in chemical concentration and/or degree of clustering considerably broaden the magnetic transition. The Curie temperature depends sensitively on the metallurgical state samples. Small gradients in chemical concentration and/or degree of chemical clustering produce a significant broadening of the ferromagnetic transition in this alloy.

2.1.1.4. PdMn alloys

The magnetic phase diagram of fcc $Pd_{1-x}Mn_x$ alloy is rather mysterious. The alloy with a Mn concentration below $x \approx 0.04$ shows ferromagnetism[34-40] although the maximum Curie temperature (T_{Curie} =7 K) appears at $x \approx 0.025$. The alloys with a Mn concentration higher than 0.05 behaves like a spin glass[38]. From experimental data[35,39,40] it follows that there is similarity of ferromagnetic $Pd_{1-x}Mn_x$ alloys with the enhanced ferromagnetic systems like $Pd_{1-x}Fe_x$ and $Pd_{1-x}Co_x$. However, in contrast to the $Pd_{1-x}Fe_x$ alloy, as the Mn concentration increases, the direct d-d interaction, which couples antiferromagnetically with the nearest-neighbor Mn-Mn pair, becomes predominant for the $Pd_{1-x}Mn_x$ alloy. The nearest-neighbor Mn-Mn pairs couple antiparallel, but the second-neighbor pairs favor ferromagnetic coupling through polarization of the conduction electrons. For the low Mn concentration alloys, the probability that two Mn atoms occupy nearest neighbor sites is very low and the ferromagnetic coupling is predominant. As the Mn concentration increases, the nearest neighbor probability increases and the conflict between firsthand second-neighbor interactions prevails. This causes the system to exhibit a spin-glass phase.

2.1.1.5. PtFe alloys

Introducing of $x \leq 0.01$ of Fe into Pt host induced a ferromagnetic range order in $Pt_{1-x}Fe_x$ alloy[41,42]. In small concentration region[41-44] up to $x \approx 0.01$, T_{Curie} depends on atomic Fe concentration x as $T_{Curie} \approx 1{,}6 \times 10^3 (x - 0.076)$ K. and characterize by the exchange integral[44] H is approximately equal to 0,14eV. At larger concentrations ($0.02 \leq x \leq 0.08$) T_{Curie} depends linear on x as $T_{Curie} \approx 20(x - 0.01)$ K. At relatively large concentrations around $x \geq 0.1$, $Pt_{1-x}Fe_x$ as well as $Pd_{1-x}Fe_x$ possess

antiferromagnetic spin correlations[46,47]. The antiferromagnetic spin component is periodically modulated and the wave vector of spin modulation varies with Fe concentration. For $Pt_{1-x}Fe_x$ alloys, an incommensurate-commensurate transition takes place around $x\approx0.14$. In[47] the concentration region around $x\approx0.1$ has been studied by neutron diffuse scattering. The scattering at 20 K was accounted for by the presence of two types of microdomains of 25 and 57A-ring radii, respectively. The magnetic moment of the larger cluster was estimated to be $\approx$ 100 μ_B. The Curie temperature and the characteristic inverse correlation length k were derived from a least-squares fit of the data to the Fischer-Burford-based expression for the scattering cross section. After correction for inelastic effects, the best estimates of the critical parameters were found to be, $T_{Curie}\approx159.5\pm0.5$K, and $k\approx0.324\pm0.015$A.

2.1.1.6. PtCo alloys.

The $Pt_{1-x}Co_x$, shows[48-54] a magnetic behavior similar to $Pd_{1-x}Fe_x$ and $Pd_{1-x}Co_x$. At low Co concentration it becomes a giant magnetic ferromagnet with critical temperatures that follows a similar pattern to that of Pd_{1-x} Fe $_x$. T_{Curie} is proportional[48,49] to $(x_C-x)^2$ for concentration $0.0066 \leq x \leq 0.01$ and proportional to x for higher concentrations of Co; critical concentration x_C equals[49] to 0,00271. At $x< x_C$ $Pt_{1-x}Co_x$ is a paramagnetic[55,56], while at larger Co concentrations $x\geq0.2$, $Pt_{1-x}Co_x$ films are hard magnetic with the magnetic moment oriented perpendicular to a substrate[56].
Summarize the data for ferromagnetic alloys with small critical concentration of ferromagnetic component we may conclude that the optimal x lays in the interval between $x\approx0.05$ and $x\approx0.15$. At larger concentration there is a finite probability for formation of the spatially inhomogeneous magnetic ordering like it is for $Pt_{1-x}Fe_x$ and $Pd_{1-x}Fe_x$ alloys. This, in turn, will give rise for generation of the triplet superconducting state[59-62] in the F-alloy with H independent decay length, exactly as it was probably observed[26] in $Nb/Pd_{1-x}Fe_x/Nb$ multilayers. At smaller concentration the ferromagnetism can be effectively suppressed due to crossover from bulk properties to the quasi two dimensional ordering in thin alloy films. The suppression of Curie temperature in thin ferromagnetic films with their thickness decrease is well known effect which occurs both for alloys and pure ferromagnet materials[63-67]. The thickness dependence of T_{Curie} and exchange energy should be the subject of the experimental study and it is one of the important unavoidable step of characterization the magnetic materials. For the case Pt and Pd based systems the rough estimation can be extracted from[26], where a factor $T_{Curie\ (bulk)}/T_{Curie(film)} \approx2\div3$ had been experimentally found in the discussed concentration range and film thickness of the order of ξ_F. Palladium is closer to ferromagnet transition compare to platinum and under the same concentration of ferromagnetic atoms has the larger Curie temperature. On the other hand Pt is to a large extend more technological material compare to Pd, which surface is very active and must be specially protected. Thus there can be some technological advantages for using $Pt_{1-x}Co_x$ or $Pt_{1-x}Fe_x$ for the SFS Josephson junction fabrication.

2.1.2. Alloys with intermediate critical concentration.

The diluted alloys $Pt_{1-x}Ni_x$, $Cu_{1-x}Ni_x$ and $V_{1-x}Fe_x$ undergoes the transition to the ferromagnetic state at $x\geq x_C\approx0.42\div0.44$ (see Fig. 2) and $x\geq x_C\approx0.25$, respectively.

2.1.2.1. PtNi alloys

Platinum and nickel can be mixed at any proportions to form a disorder solid solution having fcc structure. The disordered $Pt_{1-x}Ni_x$ alloys of composition close to $Ni_{0.75}Pt_{0.25}$ and $Ni_{0.5}Pt_{0.5}$ can be ordered by a suitable heat treatment. The disordered $Pt_{1-x}Ni_x$ alloys reach with Ni are ferromagnetic. Their Curie temperature and spontaneous magnetization increase with atomic concentration of nickel (see the data from[68-73] in Fig.1). According to[68] the critical concentration for appearance magnetism is close to $x_C\approx0.42$, while from[69] it follows that $x_C\approx0.44$. In the vicinity of critical concentration the square of Curie temperature is roughly proportional to nickel content[72] x.

2.1.2.2. CuNi alloys

The $Nb/Cu_{1-x}Ni_x/Nb$ structures with $x\approx0.54$ was historically the first, in which transition from 0-phase to π phase state was demonstrated on the temperature dependencies of the Josephson junction critical current[74,75]. The $Cu_{1-x}Ni_x$ is a weak ferromagnetic with onset of ferromagnetism at $x_C\approx0.43$. Magnetic properties and $T_{Curie}(x)$ dependencies of this compound were studied in[76,77] is shown in Fig.2. It is very closed to that for $Pt_{1-x}Ni_x$ alloy and T_{Curie} is also grows linear with x in the vicinity of x_C. The experimental data obtained in[76] for $Nb/Cu_{1-x}Ni_x$ multilayers with $x\approx0.54$ has been fitted[78] by the predictions of theoretical model based on solution of the Usadel equations resulting in $\gamma\approx0.15$, $\gamma_B\approx0.3$

and $H\approx130$ K. It is important to note that $Cu_{1-x}Ni_x$ alloy is a well studied materials, e.g. the dependencies of resistivity and spin diffusion length for this materials as a function of Ni concentration can be found in[79,80].

2.1.2.3. VFe alloys

Aarts et al[81] were the first who suggest to change the decay length in ferromagnet by varying the concentration of Fe in $V_{1-x}Fe_x$ alloy and shed the light on the important role of the SF-interface transparency in the proximity effect between S and F materials. In[81] three different sets of multilayers with alloy compositions x=1, 0.88, 0.77, 0.53, 0.38, and 0.34 were prepared. One set was used to determine μ_F, built as follows: $d_{Vout}/N[(d_{Vin}/d_F\})]/d_{Vout}$. The outer V layers d_{Vout} are for protection, typically 10-40 nm. The inner V layer d_{Vin} is typically 3 nm; it is not superconducting but meant to increase the number of interfaces, in order to obtain a realistic picture of the F layer magnetism. The F layer d_F is varied in thickness, typically between 0.5 and 5 nm, while the number of repetitions N is adapted to the strength of the moment. For Fe, N=3 suffices, while N=20 for $V_{66}Fe_{34}$. The magnetization M was measured with a magnetometer based on a superconducting quantum interference device at 5 or at 10 K. In all cases, M versus d_F could be described with a straight line, yielding the effective magnetic moment per Fe atom μ_F and the magnetically dead layer per interface d_{md}. The critical concentration is around $x_C\approx0.25$. The decay length in ferromagnet was determined experimentally from study the dependence of the critical temperature of $Nb/V_{1-x}Fe_x/Nb$ multilayer on d_F. At small d_F two Nb are stongly coupled, while with d_F increase T_C changes exponentially with d_F arriving at T_C of individial Nb in the large d_F limit. Thus defined, the concentration dependence of $\xi_F(x)$ is appeared to be proportinal to $\mu_F^{-1}(x)$, as it follows from the clean limit formular for $\xi_F = h v_F/H$. Two important consequences follow from this fact. The first is that the exchange energy $H(x)$ is proportional to $\mu_F(x)$, hence from the experimental curve $\mu_F(x)$ the values of $H(x)$ can be found if the exchange energy for pure ferromagnetic metal (x=1) is known. The second point is that the value of $H(x=0.34)\approx0.125$ meV is too large to use the theoretical predictions based on Usadel equations for the data interpretation. The last statement correlates with the analogous conclusion made in[82]. The main disadvantage of alloys with intermediate concentration of magnetic atoms is extremely small electron mean free path l. This small l gives rise to rather small decay length of these materials even in the absence of magnetic order.

2.1.3. Intermetallic compound NiAl

The intermetallic Ni_3Al compound has received extensive attention owing to its potential applications in high-temperature structural materials[83]. The unique properties of the Ni_3Al compound are principally attributed to the nature of its electronic and atomic structures. For examples, it is known[83-89] that all of Ni_3Al, which have been of great interest as a strengthener in Ni-based superalloys, have an increasing strength with increasing temperature. Ni_3Al has excellent corrosion and oxidation resistance in a wide range of temperatures owing to formation of a stable surface alumina oxide layer. Also, all of Ni_3Al, have strongly stable chemical and phase stability up to high temperatures close to their melting points. It is well known that the atomic structure of Ni_3Al has a cubic LI2-type order. In it Al occupies the cubic corners and Ni occupies the face centers so that each Ni atom is coordinated with 8 Ni and 4 Al atoms in the first shell. Electronic structure of Ni_3Al has been extencively calculated[90-92] and well known now. The magnetic properties of Ni_3Al have been studied extensively[93-102]. It has been found that in a relatively narrow composition range (x=0.735-0.76) the Ni_3Al alloys order in the Cu_2Au crystal structure and exhibit remarkable magnetic properties. In the x=0.735-0.746 Ni composition range alloys are paramagnetic whilst those with higher nickel content, with a ferromagnetic moment and Curie point which vary continuously with composition. This observation, the temperature dependence of the magnetization curves and the large high-field differential susceptibility of these ferromagnetic alloys all suggest that these systems behave like weak itinerant ferromagnets. Figure 1 gives the Curie temperature of Ni_3Al against Ni concentrations from[93-102]. Ni_3Al forms a single-crystalline layer and can exhibit a heteroepitaxial relation of being deposited on Nb. The nucleation mode is induced by a positive surface energy balance, when $\Delta\gamma_n = \gamma_{fn}+\gamma_{in}-\gamma_s>0$, where $\gamma_{fn}\approx2.08$ J/m² is the thin film surface energy for a monolayer[103,104], $\gamma_{in}\approx1.2$ J/m² is the interface energy[105] and $\gamma_s\approx3.0$ J/m² is the Nb- substrate surface energy[106]. Thus the three-dimensional epitaxial island growth corresponding to a Volmer-Weber (VW) regime[107] can be realized during the deposition process giving rise to a fiber textured Ni_3Al layer on Nb. The surface energy mismatch, $\gamma_{sf}=2|(\gamma_s-\gamma_f)/(\gamma_s+\gamma_f)|$, is equal to 0.36. The critical value defined for the formation of a superlattice structure[108] is $\gamma_{sf}=0.5$. Therefore, the growth of a superlattice structure is energetically favored. Ni_3Al can be deposited both by magnetron sputtering[109] and by the pulsed laser deposition technique[110]. The intermetallic Ni_3Al, easily oxidizes, forming a continuous coherent Al_2O_3 film (about 5 A thick) (see Ref.[111] for a review). This property is widely used in growing well-ordered alumina films for experimental investigation; for that purpose NiAl is better suited than pure Al, as the low melting temperature of the latter makes it impossible to obtain films of well-ordered alumina in

its stable configuration[111]. In particular, Al_2O_3/NiAl(110) is considered to be one of the most convenient model systems for experimental studies of alumina supported metallic nanoclusters[112]. The structure of the oxide film on the NiAl(110) surface is described as follows: at low temperatures the film is amorphous (locally ordered), at higher temperatures (about 1300 K) it becomes globally ordered and takes on the structure of two O-Al bilayers, terminated with an Al layer on the interface and with an O layer from vacuum[113-115]. According to[115], the NiAl- Al_2O_3 interface is atomically sharp without any intermediate phases. The possibility of Ni-O bond formation in either low temperature or high-temperature oxide is doubted[114-116]. The presence of "metallic" Ni at the oxidized surface at low temperatures has not been ruled out, but during the higher temperature annealing Ni atoms are suggested to be expelled from the ordering oxide overlayer[114]. All the facts discussed above give strong arguments that Ni_3Al looks very promising for SF/FS tunnel junction fabrication, while Pt based ferromagnetic alloys and the alloys with intermediate critical concentration are more suitable for weak link Josephson junction of a constriction or variable bridges types and SNS double barrier devices, respectively .

3. INTERFACES.

In the developed description of the SF/FS Josephson structures the properties of interfaces has been characterized in terms of suppression parameters[1-3] γ and γ_B

$$\gamma_B = A_B \frac{2}{3}\frac{\ell_F}{\xi_F\langle D/(1-D)\rangle}, \quad \gamma = \frac{\rho_S\xi_S}{\rho_F\xi_F} = \frac{N_F}{N_S}\sqrt{\frac{D_F}{D_S}}, \quad \xi_{S(F)} = \sqrt{\frac{D_{S(F)}}{\pi T_C}} \tag{1}$$

for the structure with finite thickness of the F-layes and γ_M, γ_{BM}

$$\gamma_{BM} = \gamma_B\frac{d_F}{\xi_F} = 2A_B\frac{\pi T_C d_F}{v_F\langle D/(1-D)\rangle}, \quad \gamma_M = \gamma\frac{d_F}{\xi_F} = \frac{N_F}{N_S}\sqrt{\frac{\pi T_C d_F^2}{D_S}}, \tag{2}$$

in the limit of small d_F. Here ℓ_F is electron mean free path in the F metals, $D_{S(N)}$, $N_{S(F)}$ and $\rho_{S(F}$ are the S(F) layer diffusion coefficients, density of states at the Fermy level and the resistivity of S(F) metals, D is interface transparency coefficient and v_F is Fermy velocity of ferromagnet.

In the free gas model the values of these parameters can be calculated making use of the bulk values for material and transport constants for the metals in proximity systems. This approach, however, gives the values considerably smaller than they are in the real experimental situation. For atomically shap clean interface the 50% mismatch of metals Fermy velocity gives $\gamma_B \approx 10^{-2}$, while experimental values[117-122] for Nb/Al, and Nb/Cu, gives $\gamma_B \approx 1$. The situation at FS interfaces even more complex then at the boundaries between the normal metals[123].

Even for weak ferromagnetic materials more exact approach[124] should take into account that close to the interface, the scattering states consist of Bloch states propagating to and away from the boundary plus evanescent contributions that decay exponentially with distance from the interface. The transmission and reflection probabilities are just the flux in the transmitted and reflected Bloch states divided by the flux in the incident Bloch state. Under this approach, in contrast to one based on free electron model, the symmetry of the states on the both sides of the interface begins to be important and interface transparency begins to be spin dependent even for weak ferromagnets. The different wave function symmetry on both sides of the barrier results also in different decay length for the plane wave inside the barrier[124-127]. The basic physical reason of this effect is that they have different amounts of curvature in the plane parallel to the interfaces. States that are primarily *s*-like will have little of this curvature, *p*-like states will have more and *d*-like states will typically have even more. This additional curvature of the wave function causes an increase in the rate of decay perpendicular to the interface. For this reason the nature of the state in the electrode influences its decay rate in the barrier is quite general. Most of the *d*-states, in particular, will be disadvantaged in penetrating the barrier because of their higher curvature due to additional nodes parallel to the barrier. The free-electron model fails to describe this aspect of real metals because it does not include spatial variations in the lateral directions (other than those associated with the lateral components of the wave vector, $k_{||}$).

The interface roughness in FS structures also becomes the very important factor. In NS proximity systems material constants of N metal relax at a distances of the order of several unit cells in the vicinity of interface, while the electron mean free path and decay length of the metals, as a rule, is macroscopically large in this scales. Thus only small corrections to parameter γ can be expected due to lattice parameter relaxation at the NS interfaces. Contrary to that in FS bilayers finite roughness results in generation of the magnetically "dead" layer at the boundary. The thickness d_{md} of this layer depends on the quality of interfaces and ferromagnet metals and typically is in the range[63-65, 128-139] 3-20 A. The structure of magnetically dead layer depends also on the degree of solubility of the F and S materials, but in all cases

with a large probability they can possess the magnetic moments in paramagnetic phase, the fact leading to additional reduction of superconductivity induced into ferromagnetic metal.
Taking into account of the fact that d_{md} is of the order of interface roughness, the parameter that experimentally can be made thin in the scales of ℓ_F and ξ_F, it is possible to describe this additional suppression channel considering the suppression parameters γ and γ_B as phenomenological values. In this approach the difference between the experimentally determined suppression parameters and the values followed from expressions (1), (2) had been use in theory should be attributed to the properties of the dead layer, thus providing indirect additional information about the structure of SF boundaries. Alternative approach is to consider the more sophisticated theoretical descriptions of SF interfaces[140-143].

4. TEORETICAL DESCRIPTION OF THE PROPERTIES OF SFS JUNCTIONS

Although the existing theories[1-3] provides rather good qualitative description of the effects observed in SFS strustures, there is still no complete quantitative agreement with experiments. This and the performed above analysis of the material and interfaces aspects indicate that besides the exchange field, some additional pair-breaking mechanisms are present in the F layers. Indeed, because of magnetic impurities, spin-wave or non stoichiometric lattices spin-flip process is inherent to the ferromagnetic layers. This may have dramatic consequences on superconductivity (contrary to non magnetic impurities that have very little impact). Such a pair-breaking mechanism also arises in usually used weak ferromagnetic alloys, because they are close to ferromagnetism disappearance and then quite favorable to large magnetic disorder. This can be inferred for instance from the very strong decrease of the critical current of S/F/S junctions as a function of the thickness of the ferromagnetic layer in resent experimental studies[144,145].
The problem of quantitative description of the influence of spin-flip and spin-orbit scattering mechanisms on critical current I_c of S/F multilayered systems had been studded only recently[146-148]. In[148] a symmetric S/F/S structure with the F layer having thickness d_F has been considered in the frame of Usadel equations[149]. Supposing that the rigid boundary conditions ($\gamma_B \gg \gamma$) are fulfilled at SF interfaces it has been shown that the expression for the critical current depends on relation between the exchange energy H and effective spin orbit scattering rate τ_{so}.
In the limit of strong spin-orbit scattering $1/\tau_{so} \geq H$, the critical current decays monotonically with the increase of d_F

$$\frac{e\xi_F \rho_F I_c}{2\pi T_c} = \frac{T}{T_c}\sum_{\omega=0}^{\infty} \frac{\Delta^2 G_S^2}{\omega^2(1+\eta_\omega^2)}(\kappa_+ + \eta_\omega^2 \kappa_-), \quad \kappa_\pm = \frac{\xi_F k_\pm}{(\gamma_B^2 \xi_F^2 k_\pm^2 + G_S^2)\sinh(k_\pm d_F) + 2G_S \gamma_B \xi_F k_\pm \cosh(k_\pm d_F)}, \tag{3}$$

$$G_S^2 = \frac{\Delta^2}{\Delta^2+\omega^2}, \quad \eta_\omega = \frac{\alpha_{so} + \sqrt{\alpha_{so}^2 - 1}}{iHsign(\omega)}, \quad k_\pm = \frac{1}{\xi_F}\sqrt{\frac{\omega}{H} + \alpha_{so} + \alpha \pm \sqrt{\alpha_{so}^2 - 1}}, \quad \alpha_{so} = \frac{1}{\tau_{so} H}, \quad \alpha = \frac{1}{\tau_m H}, \tag{4}$$

with two decay lengths $(k_\pm)^{-1}$ defined by Eq.(4). Here Δ is the magnitude of the order parameter in superconductors, $\omega = \pi T(2n+1)$ are Matsubara frequencies and τ_m is spin flip scattering rate. It is seen from (3) that in the limit $H \to 0$, the parameter $\eta_\omega \to \infty$. As a result, the contribution to the critical current in (3) comes only from κ_- component with the length scale $(k_-)^{-1}$ which describes the case of an S/N/S junction in which spin-orbit scattering does not influence I_c. With the increase of H, the contribution to I_c from the faster decaying κ_+ component ($k_+ > k_-$) also increases and the difference between k_- and k_+ decreases. Finally, when $H = (\tau_{so})^{-1}$, both scales coincide, $k_+ = k_-$, and the components κ_+, κ_- provide equal contributions to I_c. For relatively weak spin-orbit scattering, $(\tau_{so})^{-1} \leq H$, the dependence $I_c(d_F)$ follows the damped oscillation law,

$$\frac{e\xi\rho_F I_c}{2\pi T_c} = \frac{T}{T_c}\sum_{\omega=0}^{\infty} \frac{\Delta^2 G_S^2}{\omega^2(1+\eta_\omega^2)} \mathrm{Re}\left\{\frac{(a+ib)\left[1 + 2i/\sqrt{\alpha_{so}^{-1} - 1}\right]}{(\gamma_B^2 \xi_F^2 k^2 + G_S^2)\sinh(qd_F/\xi) + 2G_S \gamma_B \xi_F k \cosh(qd_F/\xi)}\right\}, \quad \xi = \sqrt{\frac{D_F}{H}}, \tag{5}$$

$$a = \sqrt{\frac{\omega}{H} + \alpha_{so} + \alpha + \sqrt{\left(\frac{\omega}{H} + \alpha\right)^2 + 2\alpha_{so}\left(\frac{\omega}{H} + \alpha\right)} + 1}, \quad b = \frac{\sqrt{1 - \alpha_{so}^2}}{a}, \quad q = a + ib, \tag{6}$$

when two length scales ξ_1, ξ_2 can be introduced describing respectively the decay and the oscillation period of $I_c(d_F)$. The existence of these two scales is clearly form the results of numerical calculations presented in Fig.3,4. The calculations performed for $H = 3\pi T_c$, $\gamma_B = 10$, $T/T_c = 0{,}5$ and different values of spin flip (Fig.3, $\alpha_{so} = 0$) and spin orbit

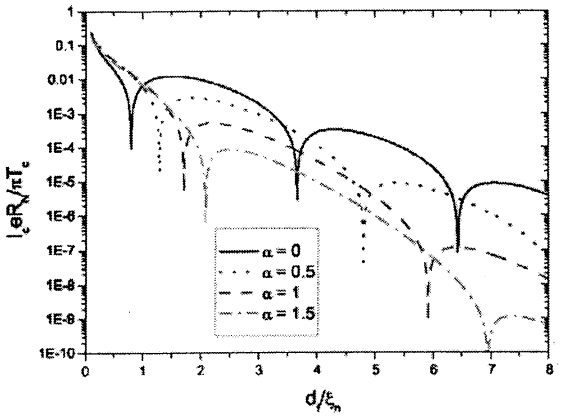

Figure 3: Influence of the spin-flip scattering parameter α on the thickness dependence of the critical current in S/F/S junction for $\alpha_{so} = 0$; $H = 3\pi T_c$, $\gamma_B = 10$, and $T/T_c = 0{,}5$.

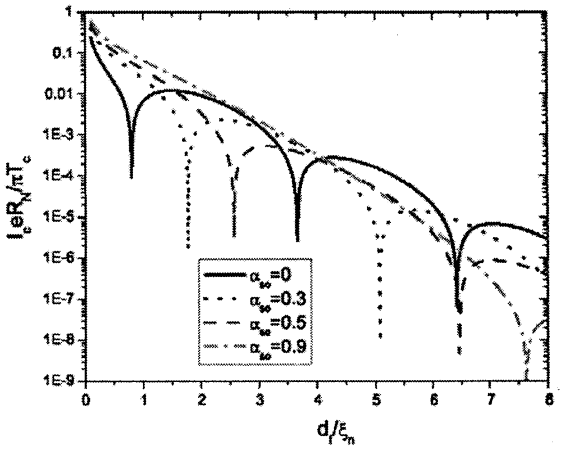

Figure 4: Influence of the spin-orbit scattering on the thickness dependence of the critical current in S/F/S junction for $\alpha = 0$, $H = 3\pi T_c$, $\gamma_B = 10$, and $T/T_c = 0{,}5$.

(Fig.4, $\alpha = 0$) scattering rates. From the calculations it follows that spin-flip and spin-orbit scattering lead to the decrease of the decay length and the increase of the oscillations period. It is seen also that the oscillation period increases strongly with increasing α_{so} and diverges when $\alpha_{so} = 1$. Therefore spin-orbit and spin-flip scattering mechanisms influence differently the properties of S/F structures: spin-orbit mechanism can destroy the $I_c(d_F)$ oscillations while spin-flip scattering can only modify them. The obtained analytical and numerical solutions of the problem provide the basis not only for qualitative understanding of experimental results but also to fit the data quantitatively.

At the point of 0-π transition the critical current of SFS structures equals to zero, or, more exactly, the amplitude I_c of $\sin(\varphi)$ component in the supercurrent is equal to zero. From general considerations[1] it follows that under this condition the next, say $\sin(2\varphi)$, term starts to be important and fully determines the $J(\varphi)$ curve. In[150] it has been shown that there are two different physical mechanisms that are responsible for the sign of $J_{12}\sin(2\varphi)$. The first one is the depairing by current which contributes positively to the $\sin(2\varphi)$ term, while the second one is the finite transparency of SF interfaces which provides the negative contribution. The physical reason for different signs of J_{12} can be easily understood if we consider the SFIFS tunnel junctions and analyze the two cases separately. Suppose first that suppression parameter at SF interfaces γ_B is finite. In this case the SFIFS structure may be considered as a system of three Josephson junctions in series as shown schematically in Fig.5. For rough estimates one can assume that the phase χ of anomalous Green's functions Θ does not depend on ω. Demanding the equality of the currents across FIF and FS interfaces and taking into account that critical currents $I_c \sim 1/\gamma_{BI}$ of FIF and $I_{c1} \sim 1/\gamma_B$ of FS interfaces are essentially different ($I_c \ll I_{c1}$) for effective phase of Green's functions in the F layer χ and $J(\varphi)$ we get

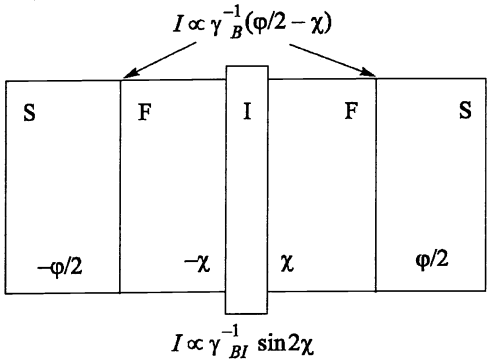

Figure 5: The phase distribution in SFIFS junction

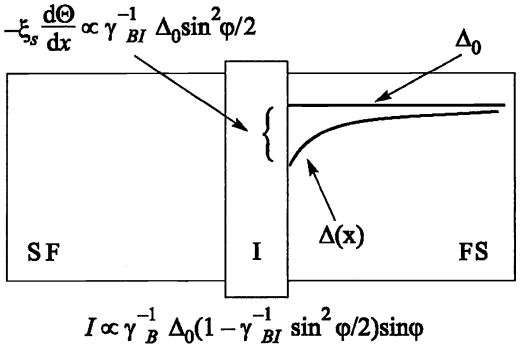

Figure 6: Depairing by current near the tunnel barrier.

$$I_c \sin 2\chi = I_{c1} \sin(\chi - \frac{\varphi}{2}) \approx I_{c1}(\frac{\varphi}{2} - \chi),\ \chi \approx \frac{\varphi}{2} - \frac{I_c}{I_{c1}} \sin\varphi,\ I = I_c \sin 2\chi = I_c \sin\left(\varphi - \frac{2I_c}{I_{c1}} \sin\varphi\right) \approx I_c\left(\sin\varphi - \frac{I_c}{I_{c1}} \sin 2\varphi\right)$$

Therefore with increasing γ_B the phase partly jumps at the FS interfaces leading to a continuous crossover from the Josephson effect lumped at FIF interface (x=0) to the phase drop distributed at $|x| \leq d_F$. In a full agreement with the theory of double barrier devices[1] this crossover results in appearance of second harmonic in $J(\varphi)$ with negative sign which provides maximum $J(\varphi)$ achieved at $\varphi \geq \pi/2$. If γ_B=0, the structure is always lumped at x=0 and the main effect is the suppression of superconductivity by supercurrent in the vicinity of FIF interface as shown schematically in Fig.6. The resulting contribution to the full current can be estimated by taking into account that the order parameter slightly suppressed at FIF by a current. This suppression is described by gradient term in the brackets in (7). Its value follows from the boundary conditions for anomalous Green's functions Θ at FIF interface (see Ref.[150] for the details)

$$I \propto \frac{1}{\gamma_{BI}}\left(\Delta - \xi \frac{d}{dx}\Theta\right)\sin\varphi \propto \frac{\Delta}{\gamma_{BI}}\left(1 - \frac{\sin^2(\varphi/2)}{\gamma_{BI}}\right)\sin\varphi \approx \frac{\Delta}{\gamma_{BI}}\left(\sin\varphi + \frac{\sin(2\varphi)}{4\gamma_{BI}}\right) \quad (7)$$

It follows directly from (7) that the amplitude of the second harmonic is positive. The developed in[150] analytical method for solution of linearized Usadel equations permits to solve the problem of $J(\varphi)$ determination selfconsistently and fully confirm the results of this simple qualitative considerations.

5. CONCLUSION

We review the material and interfaces aspects of the problem of SFS Josephson junction fabrication. Our analysis has shown that in order to have a ferromagnetic material with reasonably large decay length we should not only to suppress the exchange energy, as it is in delude F alloys, but within the limits of the possible do not suppress the electron mean free path. The last may be achieved either in alloys with Pt or Pd hosts in which no more than several atomic percent of magnetic atoms is enough for nucleation of the desire ferromagnetic state or by using intermetallic metals like Ni_3Al. Nevertheless, in both approaches it is difficult to control the homogeneity of spatial distribution of ferromagnetic atoms in the host material during the fabrication process. This, in turn, should result in switching on of additional pair breaking mechanisms both at SF interfaces (like a dead layer) and in the bulk provided by spin flip and spin orbit scattering. We also present here the results of calculations in the frame of microscopic theory of superconductivity, which take into account these effects and provide good bases for the data interpretations.

This work has been supported in part by Russian Ministry of Education and Science, RFBR Grant N 04 0217397-a, INTAS Grant 01- 0809, NWO-RFBR cooperation programme 047.016.005 and ESF PiShift programme.

6. REFERENCES

1. A.A. Golubov, M.Yu. Kupriyanov, E. Il'ichev, Rev.Mod.Phys, **76**, 411-469 (2004).
2. A.I. Buzdin, Rev.Mod.Phys, **77**, 935-976, (2005).
3. F.S. Bergeret, A.F. Volkov and K.B. Efetov, *Odd triplet superconductivity and related phenomena in superconductor-ferromagnet structures*, to be published in Rev.Mod.Phys., (2006).
4. J. W. Cable, E. O. Wollan, and W. C. Koehler, Phys. Rev. **138**, A755 (1965).
5. R.Segnan, Phys.Rev. **160**, 404 (1967).
6. W. A. Ferrando, R. Segnan, and A. I. Schindler, J.Appl.Phys., **41**, 1236 (1970).
7. W. A. Ferrando, R. Segnan, and A. I. Schindler, Phys. Rev. B **5**, 4657 (1972).
8. S. Crane, D. W. Carnegie, Jr., and H. Claus, J. Appl. Phys. **53**, 2179 (1982).
9. M. Nicklas, M. Brando, G. Knebel, F. Mayr, W. Trinkl, and A. Loidl, Phys. Rev. Lett. **82**, 4268 (1999).
10. A. P. Murani, A. Tari, and B. R. Coles, J. Phys. F **4**, 1769 (1974).
11. J.Grangle and W.R.Scott, J.Appl.Phys., **36**, 921 (1965).
12. H.Fujiwara et al., J.Phys.Soc.Jpn., **40**,1010 (1976).
13. J.Beille and R. Tournier, J.Phys.F **6**, 621 (1976).
14. S.K.Burke et al., J.Appl.Phys., **53**, 8079 (1982).
15. T. Kontos, M. Aprili, J. Lesueur, and X. Grison, Phys. Rev. Lett. **86**, 304 (2001).
16. T. Kontos, M. Aprili, J. Lesueur, F. Genet, B. Stephanidis, and R.Boursier, cond-mat/0201104, (2002).
17. G.J. Nieuwenhuys, Adv. Phys. **24**, 515 (1975) and references therein.
18. P. A. Schroeder and C. Uher, Phys. Rev. B **18**, 3884-3889 (1978).
19. R. Medina and R. E. Parra, Phys. Rev. B **26**, 5187 (1982).

20. J. R. Long and R. W. Mattozzi, Journal of Applied Physics, **55**, 2359 (1984).
21. C. A. Kuhnen and E. Z. da Silva, Phys. Rev. B **46**, 8915 (1992).
22. C. Büscher, T. Auerswald, E. Scheer, A. Schröder, H. v. Löhneysen, H. Claus, Phys. Rev. B **46**, 983-989 (1992).
23. P. Mohn, E. Supanetz, K. Schwarz, Aust. J. Phys. **46**, 651 (1993).
24. T. Hermannsdorfer, S. Rehmann, W. Wendler, F. Pobell, J. Low Temp. Phys. **104**, 49 (1996).
25. Soong-Hyuck Lee and D. J. Webb, Phys. Rev. B **55**, 13993 (1997).
26. M. Scho"ck, C. Surgersa, and H.v. Lo"hneysen Eur. Phys. J. B **14**, 110 (2000).
27. G.Griffith, F.A.Volkenng and H.Claus J.Appl.Phys, **57** 3392 (1985).
28. A. Pilipowicz and H. Claus, Phys. Rev. B **36**, 773 (1987).
29. R. P. Peters, Ch. Buchal, M. Kubota, R. M. Mueller, and F. Pobell, Phys. Rev. Lett. **53**, 1108 (1984).
30. K.Kornik, H.Kunkel and R.M.Roshko, J.Appl.Phys., **64**, 5619 (1988).
31. R. M. Bozortb, P. A. Wolff, D. D. Davis, V. B. Compton, and J. H. Wernick, Phys. Rev. **122**, 1157 (1961).
32. G. G. Low and T. M. Holden, Proc. Phys. Soc. London **89**, 119 (1966).
33. B. D. Dunlap and J. G. Dash, Phys. Rev. **155**, 460 (1967).
34. H. A. Zweers and G. J. van den Berg, J. Phys. F **5**, 555 (1975).
35. B. R. Coles, H. Jamieson, R. H. Taylor, and A. Tari,, J. Phys. F **5**, 565 (1975).
36. W. M. Star, S. Foner and E. J. McNiff, Jr., Phys. Rev. B **12**, 2690-2709 (1975).
37. R. E. Parra and A. C. González, J.Appl. Phys. **69**, 6138 (1991).
38. C. Ho, I. Maartense, and G. Williams Phys. Rev. B **24**, 5174 (1981).
39. G. Williams and J. W. Loram, Solid State Commun. **7**, 1261 (1969).
40. J. W. Cable and L. David, Phys. Rev. B **16**, 297 (1977).
41. J. Grangle, W.R.Scott, J.Appl.Phys., **36**, 921 (1965).
42. R.Segnan, Phys.Rev., **160**, 404 (1967).
43. J.C.Ododo, J.Phys. F, **9**,1441 (1979).
44. M.A.Jensen and K. Andres, J.Appl.Phys., **38**, 1255 (1967).
45. J. W. Loram, R. J. White, and A. D. C. Grassie, Phys. Rev. B **5**, 3659 (1972).
46. P. Radhakrishna, H. M. Gilder, G. Parette, and A. Menelle, Phys. Rev. B **40**, 2435 (1989).
47. Yorihiko Tsunoda and Ryo Abe, Phys. Rev. B **55**, 11507 (1997).
48. J.C.Ododo, J.Phys. F**12**, 1821 (1982).
49. B.Tissier, Rtouraier, Solid State Commun. **11**, 895 (1972).
50. R. E. Parra and R. A. López, J. Appl. Phys. **61**, 3989 (1987).
51. C. W. Lee, C. L. Foiles, J. Bass, and J. R. Cleveland, J. Appl. Phys. **49**, 2174 (1978).
52. Gwyn Williams, G. A. Swallow, and J. W. Loram Phys. Rev. B **11**, 337 (1975).
53. Gwyn Williams, G. A. Swallow, and J. W. Loram, Phys. Rev. B **11**, 344 (1975).
54. G. Hadjipanayis and P. Gaunt, J. Appl. Phys. **50**, 2358 (1979).
55. B. M. Lairson, M. R. Visokay, E. E. Marinero, R. Sinclair, and B. M. Clemens, J. Appl. Phys. **74**, 1922 (1993).
56. E. Beaurepaire, M. Maret, V. Halté, J.-C. Merle, A. Daunois, and J.-Y. Bigot, Phys. Rev. B **58**, 12134 (1998).
57. E. Beaurepaire, M. Maret, V. Halté, J.-C. Merle, A. Daunois, and J.-Y. Bigot, Phys. Rev. B **58**, 12134 (1998).
58. Arti Kashyap, K. B. Garg, A. K. Solanki, T. Nautiyal, and S. Auluck, Phys. Rev. B **60**, 2262 (1999).
59. M. L. Kuli´c and I. M. Kuli´c, Phys. Rev. B **63**, 104503 (2001);
60. F.S.Bergeret, A.F.Volkov, K.B.Efetov, Phys.Rev.Lett., **86** 4096 (2000).
61. A.Kadigrobov, R.I.Shekter, M.Jonson, Europhys.Lett., **54**, 394 (2001); J.Low Temp.Phys., **27** 760, (2001).
62. F.S.Bergeret, A.F.Volkov, K.B.Efetov, Phys.Rev.B., **64**, 134506 (2001).
63. Y. Obi, M. Ikebe, T. Kubo and H. Fujimori, Physica C **317 - 318** 149 (1999).
64. Th. Mühge, K. Westerholt, H. Zabel, N. N. Garif'yanov, Yu. V. Goryunov, I. A. Garifullin, and G. G. Khaliullin, Phys. Rev. B **55**, 8945 (1997).
65. Th. Mu"hge, N.N. Garif'yanov, Yu.V. Goryunov, G.G. Khaliullin, L.R. Ragirov, K. Westerholt, I.A. Garifullin, and H. Zabel, Phys. Rev. Lett. **77**, 1857 (1996);
66. Th. Mu"hge, T. Theis-Bröhl, K. Westerholt, J. Zabel, N.N. Garif'yanov, Yu.V. Goryunov, A.I. Garifullin, and G.G. Khaliullin, Phys. Rev. B **57**, 5071 (1998)
67. G. Verbanck, C.D. Potter, V. Metlusko, R. Schad, V.V. Moschalkov, and Y. Bruynseraede, Phys. Rev. B **57**, 6029 (1998).
68. M. J. Besnus and A. Herr, Phys. Lett. A **39**, 83 (1972).
69. D. J. Gillespie and A. I. Schindler, AIP Conf. Proc. **5**, 461 (1972).

70. V. Marian, Ann. Phys. 7, 514 (1937).
71. G. Fisher and M. J. Besnus, Solid State Commun. 7, 1527 (1969).
72. H. L. Alberts, J. Beille, and D. Bloch E. P. Wohlfarth, Phys. Rev. B **9**, 2233 (1974).
73. W. A. Ferrando, R. Segnan, A. I. Schindler, Phys. Rev. B **5**, 4657 (1972).
74. V.V.Ryazanov, V.A.Oboznov, A.Yu.Rusanov, V.V.Veretennikov, A.A.Golubov, J.Aarts, Phys.Rev.Lett., **86**, 2427 (2001).
75. V. V. Ryazanov, V. A. Oboznov, A. V. Veretennikov, and A. Yu. Rusanov, Phys. Rev. B **65**, 020501 (2002).
76. A. Rusanov, R. Boogaard, M. Hesselberth, H. Sellier and J. Aarts, Phys.C **369** 300 (2002).
77. S.A. Ahern, M.J.C. Martin and W. Sucksmith Proc. Royal Soc. (London) A **248** 145 (1958),.
78. Fominov : Ya. V. Fominov, N. M. Chtchelkatchev, and A. A. Golubov, Pis'ma Zh. Eksp. Teor. Fiz. **74**, 101 (2001) [JETP Lett. **74**, 96 (2001)].
79. P. A. Schroeder, R. Wolf, and J. A. Woollam, Phys. Rev. **138**, A105-A111 (1965).
80. Shih-Ying Hsu, P. Holody, R. Loloee, J. M. Rittner, W. P. Pratt, Jr., and P. A. Schroeder, Phys. Rev. B **54**, 9027 (1996).
81. Aarts : J. Aarts, J.M.E. Geers, E. Bruck, A.A. Golubov, and R. Coehoorn, Phys. Rev. B **56**, 2779 (1997).
82. Blum : Y. Blum, A. Tsukernik, M. Karpovski, A. Palevski, cond-mat/0203408 (to be published in Phys. Rev. Lett. (2002)).
83. N. S. Stoloff, Int. Met. Rev. **29**, 123 (1984).
84. D.P. Pope and S.S. Ezz, Int Mater Rev. **29** 136 (1984),.
85. N.S. Stoloff, Int Mater Rev. **34** 153 (1989),.
86. M. Yamaguchi and Y. Umakoshi Prog Mater Sic **34** 1 (1990).
87. T. Suzuki, Y. Mishima and S. Miura ISIJ Int **29** 1 (1989).
88. K. Hagiwara, T. Nakano, Y. Umakoshi, Collected Abstract of 2000 Fall Meeting of Japan Inst. Metals. p. 433.
89. K. Hagiwara, T. Nakano and Y. Umakoshi Acta Materfialia **48** 1469 (2000).
90. T. Nautiyal and S. Auluck, Phys. Rev. B **45**, 13930-13937 (1992).
91. D. A. Muller, P. E. Batson, and J. Silcox, Phys. Rev. B **58**, 11970 (1998).
92. D. A. Muller, D. J. Singh, and J. Silcox, Phys. Rev. B **57**, 8181 (1998).
93. F. R. De Boer, C. J. Schinkel, and J. Biesterbos, Phys. Lett. A**25**, 606 (1967).
94. F. R. De Boer, C. J. Schinkel, J. Biesterbos, and S. Proost, J. Appl. Phys. **40**, 1049 (1969).
95. N. Buis, J. J. M. Franse and P. E. Brommer, Physica B&C **106B**, 1 (1981).
96. H. Sasakura, K. Suzuki, and Y. Masuda, J. Phys. Soc. Jpn. **53**, 352 (1984).
97. H. Sasakura, K. Suzuki, and Y. Masuda, J. Phys. Soc. Jpn. **53**, 754 (1984).
98. S. Takahashi, A.Y. Takahashi, and A. Chiba, J. Phys.: Condens. Matter **6**, 6011 (1994).
99. Yoshizawa M, Seki H, Ikeda K, Okuno K, Saito M and Shigematsu K, J. Phys. Soc. Japan **61**, 3313 (1992).
100. S Takahashi, A Chiba and A Y Takahashi, J. Phys.: Condens. Matter. **6**, 10795 (1994).
101. S. K. Dhar, K. A. Gachneidner, Jr., L. L. Miller and D. C. Jonston, Phys. Rev. B **40** 11488 (1989).
102. K.Suzuki, Y.Masuda, J.Phys.Soc.Jpn., **53**, 754 (1984).
103. Y. Du and N. Clavaguera, J. Appl. Cryst. **237** 20 (1996).
104. W. Huang and Y.A. Chang, Intermetallics **6** 487 (1998).
105. G. Lu and N. Kioussis. MRS Symp. Proc. **472** 21 (1997).
106. F. J. Himpsel, J. E. Ortega, G. J. Mankey and R. F. Willis , Advances in Physics, **47**, 511 (1998).
107. D.L. Smith. Thin-Film Deposition: Principles and Practice, McGraw-Hill, New York (1995).
108. E. Bauer and J.H. van der Merwe. Phys. Rev. B **33** 3657 (1986).
109. P. de Almeida, R. Scha"ublin, A. Almazouzi, M. Victoria and F. Le'vy, Thin Solid Films, **368**, 26 (2000).
110. R. K. Singh, Deepika Bhattacharya, S. Sharan, P. Tiwari, J. Narayan, Journal of Materials Research, **7**, 2639 (1992).
111. H.-J. Freund, H. Kuhlenbeck, and V. Staemmler, Rep. Prog. Phys. **59**, 283 (1996).
112. K. H. Hansen et al., Phys. Rev. Lett. **83**, 4120 (1999).
113. J. Libuda et al., Surf. Sci. **318**, 61 (1994).
114. R. M. Jaeger et al., Surf. Sci. **259**, 235 (1991).
115. J. C. Yang, E. Schumann, H. Mu"llejans, and M. Ru"hle, J. Phys. D **29**, 1716 (1996).
116. H. Isern and G. R. Castro, Surf. Sci. **211-212**, 865 (1989).
117. P.N. Dmitriev, A.B. Ermakov, A.G. Kovalenko, V.P. Koshelets, N.N. Iosad, A.A. Golubov, M.Yu. Kupriyanov, IEEE Tran.Applied Superconductivity, **9** 3970 (1999).

118. A. Zehnder, Ph. Lerch, S.P. Zhao, Th. Nussbaumer and E.C. Kirk, Phys.Rev. B **59** 8875 (1999).
119. G. Brammertz, A. Poelaert, A. A. Golubov, P. Verhoeve, A. Peacock, and H. Rogalla J. Appl. Phys. **90**, 355 (2001).
120. G. Brammertz, A. Golubov, A. Peacock, P. Verhoeve, D. J. Goldie and R. Venn, Physica C **350**, 227 (2001).
121. W. Park, D. V. Baxter, S. Steenwyk, I. Moraru, W. P. Pratt, Jr., and J. Bass Phys. Rev. B **62**, 1178 (2000).
122. D. V. Baxter et al., J. Appl. Phys. **85**, 4545 (1999).
123. K. Xia, P. J. Kelly, G. E. W. Bauer, A. Brataas, and I. Turek, Phys. Rev. B **65**, 220401 (2002).
124. M. D. Stiles, J.Appl.Phys., **79**, 5805 (1996).
125. J. M. MacLaren, X.-G. Zhang, W. H. Butler, and Xindong Wang, Phys. Rev. B **59**, 5470 (1999).
126. W. H. Butler, X.-G. Zhang, T. C. Schulthess, and J. M. MacLaren, Phys. Rev. B **63**, 054416 (2001).
127. W. H. Butler, X.-G. Zhang, and T. C. Schulthess J. M. MacLaren, Phys. Rev. B **63**, 092402 (2001).
128. C. Strunk, C. Su"rgers, U. Paschen and H.v. Lo"hneysen, Phys. Rev. **49** 4053 (1994).
129. G. Verbanck, C. D. Potter, R. Schad, V. V. Moshchalkov, and Y. Bruynseraede, Phys. C, **235-240** 3295 (1994).
130. Th. Mu"hge, N.N. Garif'yanov, Yu.V. Goryunov, K. Theis-BrO"hl, K. Westerholt, I.A. Garifullin, and H. Zabel, Physica C **296**, 325 (1998)
131. J. E. Mattson, C. H. Sowers, A. Berger, and S. D. Bader, Phys. Rev. Lett. **68** 3252 (1992).
132. .E. Mattson, R.M. Osgood III, C.D. Potter, C.H. Sowers and S.D. Bader. J. Vac. Sci. Technol. A **15** 177 (1997).
133. E. Navarro, J. E. Villegas and J. L. Vicent, Journal of magnetism and Magnetic Materials, **240** 586 (2002).
134. S. F. Lee, Y. Liou, Y. D. Yao, W. T. Shih, and C. Yu, J.Appl.Phys., **87**, 5564 (2000).
135. S. F. Lee, T. M. Chuang, S. Y. Huang, W. L. Chang, and Y. D. Yao, J.Appl.Phys., **89**, 5463 (2001).
136. Antony Ajan, Shiva Prasad, R. Krishnan, N. Venkataramani, and M. Tessier, J.Appl.Phys. **91**, 1444 (2002).
137. P. Koorevaar, Y. Suzuki, R. Coehoorn and J. Aarts. Phys. Rev. B **49** 441 (1994).
138. P. Koorevaar, Y. Suzuki and J. Aarts. Physica C **248** 61 (1995).
139. L. R. Tagirov, I. A. Garifullin, N. N Garif'yanov, S. Ya. Khlebnikov, D. A. Tikhonov, K. Westerholt and H. Zabel, Journal of Magnetism and Magnetic Materials, **240** 577 (2002).
140. M. Fogelström, Phys. Rev. B **62**, 11812 (2000).
141. J. C. Cuevas and M. Fogelström, Phys. Rev. B **64**, 104502 (2001).
142. M. Eschrig, J. Kopu, J. C. Cuevas, and Gerd Schön, Phys. Rev. Lett. **90**, 137003 (2003).
143. A. I. Buzdin, A. V. Vedyayev and N. V. Ryshanova, Europhys. Lett. **48**, 686 (1999).
144. H. Sellier, C. Baraduc, F. Lefloch, and R. Calemczuck, Phys. Rev. B **68**, 054531 (2003).
145. V. A. Oboznov, V. V. Bol'ginov, A. K. Feofanov, V. V. Ryazanov, and A. Buzdin, cond-mat/0508573.
146. V. N. Krivoruchko and R. V. Petryuk, Phys. Rev. B **66**, 134520 (2002).
147. F. S. Bergeret, A. F. Volkov, and K. B. Efetov, Phys. Rev. B **68**, 064513 (2003).
148. M. Fauré, A. I. Buzdin, A. A. Golubov, M. Yu. Kupriyanov, Striking properties of Superconductor/Ferromagnet structures with spin-dependent scattering, submitted to PRB (2006).
149. L. Usadel, Phys. Rev. Lett. **25**, 507 (1970).
150. A. A. Golubov, and M. Yu. Kupriyanov, Pisma ZhETF, **81** 419 (2005).